Stable Ring-Profile Vortex Solitons in Bessel Optical Lattices

Yaroslav V. Kartashov,[1,2] Victor A. Vysloukh,[3] and Lluis Torner[1]

[1]*ICFO-Institut de Ciencies Fotoniques, and Department of Signal Theory and Communications, Universitat Politecnica de Catalunya, 08034, Barcelona, Spain*

[2]*Physics Department, M. V. Lomonosov Moscow State University, 119899, Moscow, Russia*

[3]*Departamento de Fisica y Matematicas, Universidad de las Americas–Puebla, Santa Catarina Martir, 72820, Puebla, Mexico*

(Received 30 June 2004; published 3 February 2005)

Stable ring-profile vortex solitons, featuring a bright shape, appear to be very rare in nature. However, here we show that they exist and can be made dynamically stable in defocusing cubic nonlinear media with an imprinted Bessel optical lattice. We find the families of vortex solitons and reveal their salient properties, including the conditions required for their stability. We show that the higher the soliton topological charge, the deeper the lattice modulation necessary for stabilization.

DOI: 10.1103/PhysRevLett.94.043902 PACS numbers: 42.65.Tg, 42.65.Jx, 42.65.Wi

Vortex solitons with a bright shape, i.e., screw topological phase dislocations embedded in a localized ring-shaped beam, might exist in different systems with focusing nonlinearities [1]. However, such solitons realize higher-order, excited states of the corresponding nonlinear systems; therefore, they tend to be highly prone to azimuthal modulational instabilities that lead to their spontaneous self-destruction into ground-state solitons [2]. This process has been observed experimentally in different settings [3]. Homogeneous defocusing nonlinear media can support stable vortex solitons, but those have the form of dark-shaped beams [4]. Localized, stable ring-vortex solitons in homogeneous media are known to exist in models with competing cubic-quintic or quadratic-cubic nonlinearities [5,6]. Nevertheless, such models are very challenging to implement in practice, as they require very large light intensities where the higher-order nonlinearities are typically accompanied by additional dominant processes, like multiphoton absorption [7]. Successful alternatives are confined systems, such as graded-index optical fibers [8], trapped Bose-Einstein condensates [9], or nonlinear photonic crystals with defects [10], where stabilization of the ring-shaped beam is induced by the corresponding confining potentials.

In this Letter we introduce a new approach to form stable nonlinear, ring-profile vortices which is based on the concept of *Bessel optical lattices.* It is known that spatial modulation of the refractive index profoundly affects soliton properties [11–13]. It was demonstrated recently that optical lattices with tunable refractive-index modulation depth and period can be induced optically in photorefractive materials [14–17]. To date, efforts have been devoted to the investigation of solitons supported by lattices with a honeycomb symmetry that are induced by intersecting plane waves [14–18]. However, Bessel lattices with a radial shape are also possible [19]. Importantly, the Bessel concept provides *localized* refractive-index modulations, in contrast to the extended shape of honeycomb lattices. Here we address Bessel lattices imprinted in defocusing cubic nonlinear media and uncover the properties of higher-order excited vortex soliton states supported by the structure. We show that vortex lattice solitons (VLS) exist in these lattices and that they can be made dynamically stable with suitable lattice strength. The VLS are the nonlinear continuation of the lattice modes, but, in contrast to such modes, VLS might extend over several lattice rings, thus featuring a multiring bright shape.

We consider light propagation along the z axis in a bulk medium with the defocusing cubic nonlinearity and transverse modulation of the refractive index described by the

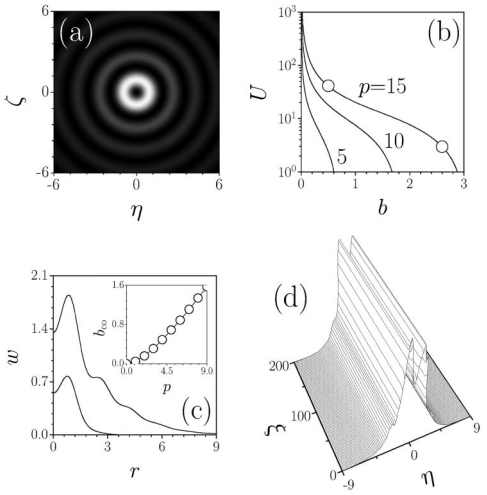

FIG. 1. (a) First-order Bessel lattice. Regions with higher refractive index are shown with white color; regions with lower refractive index are shown with black color. (b) Power of ground-state soliton versus the propagation constant. (c) Amplitude profiles of solitons corresponding to points marked by circles in (b) at $p = 15$. Inset in (c) shows upper cutoff versus lattice depth. (d) Stable propagation of the ground-state soliton with $b = 0.8$ at $p = 15$ in the presence of white noise with variance $\sigma^2_{\text{noise}} = 0.01$. Cut of intensity distribution at $\zeta = 0$ is shown.

nonlinear Schrödinger equation for the normalized complex field amplitude q:

$$i\frac{\partial q}{\partial \xi} = -\frac{1}{2}\left(\frac{\partial^2 q}{\partial \eta^2} + \frac{\partial^2 q}{\partial \zeta^2}\right) + q|q|^2 - pR(\eta, \zeta)q. \quad (1)$$

The longitudinal ξ and transverse η, ζ coordinates are scaled to the diffraction length and input beam width, respectively. The parameter p is proportional to the depth of the refractive-index modulation, and the function $R(\eta, \zeta) = J_1^2[(2b_{\rm lin})^{1/2} r]$ with $r^2 = \eta^2 + \zeta^2$ stands for the transverse profile of the refractive index; the parameter $b_{\rm lin}$ is related to the radii of rings in the first-order Bessel lattice. The optical field of the lattice-creating first-order Bessel beam is given by $J_1[(2b_{\rm lin})^{1/2} r]\exp(-ib_{\rm lin}\xi + i\phi)$, where ϕ is the azimuthal angle. Such beams can be created experimentally by holographic techniques [20], while vectorial interactions in a slow Kerr-type medium (including, e.g., photorefractive crystals) can be utilized for trapping and guiding beams of orthogonal polarization in the lattice formed by the Bessel beam. We assume that the refractive-index profile is given by the intensity of the first-order Bessel beam as this case is favorable for vortex soliton formation [see Fig. 1(a)]. Equation (1) requires nonlinearities of different signs for soliton and lattice-creating beams. In principle, such experimental conditions can be met in the photorefractive semiconductor crystals such as GaAs:Cr, InP:Fe, and CdTe:In, belonging to the $\bar{4}3m$ point symmetry group [21]. These materials are transparent for near infrared wavelengths and exhibit strong photorefractivity (e.g., $n^3 r_{41} = 152$ pm/V in CdTe:In), and the sign of nonlinearity might be changed by a $\pi/2$ rotation of the polarization direction. Notice that the peak value of the photorefractive contribution to the refractive index in such crystals could reach $\sim 10^{-3}$ [that corresponds to $p \sim 10$ in Eq. (1)] provided that sufficiently strong static electric field is applied. Equation (1) admits several conserved quantities, including the power, or energy flow, $U = \int_{-\infty}^{\infty}\int_{-\infty}^{\infty} |q|^2 d\eta d\zeta$. We also stress that Eq. (1) holds for trapped Bose-Einstein condensates with repulsive interactions [9].

We search for solutions of Eq. (1) in the form $q(\eta, \zeta, \xi) = w(r)\exp(im\phi)\exp(ib\xi)$, where b is the propagation constant, m is the topological charge, and $w(r)$ is the real function. Substitution of the light field in such a form into Eq. (1) yields

$$\frac{d^2 w}{dr^2} + \frac{1}{r}\frac{dw}{dr} - \frac{m^2 w}{r^2} - 2bw - 2w^3 + 2pRw = 0, \quad (2)$$

an equation that we solved numerically with a relaxation method. Mathematically, the soliton families are defined by the propagation constant b, the lattice depth p, and the parameter $b_{\rm lin}$. Since one can use the scaling transformation $q(\eta, \zeta, \xi, p) \to \chi q(\chi\eta, \chi\zeta, \chi^2\xi, \chi^2 p)$ to obtain various families of solitons from a given one, we set the transverse scale in such way that $b_{\rm lin} = 2$ and varied b and p. To analyze the dynamical stability of the soliton families we searched for perturbed solutions with the form $q(\eta, \zeta, \xi) = [w(r) + u(r, \xi)\exp(in\phi) + \nu^*(r, \xi) \times \exp(-in\phi)]\exp(ib\xi + im\phi)$, where the perturbation components u, ν could grow with complex rate δ upon propagation, and n is the azimuthal index of the perturbation. Linearization of Eq. (1) around a stationary solution $w(r)$ yields the eigenvalue problem:

$$\begin{aligned} i\delta u &= -\frac{1}{2}\left(\frac{d^2}{dr^2} + \frac{1}{r}\frac{d}{dr} - \frac{(m+n)^2}{r^2}\right)u + bu \\ &\quad + w^2(\nu + 2u) - pRu, \\ -i\delta \nu &= -\frac{1}{2}\left(\frac{d^2}{dr^2} + \frac{1}{r}\frac{d}{dr} - \frac{(m-n)^2}{r^2}\right)\nu + b\nu \\ &\quad + w^2(u + 2\nu) - pR\nu, \end{aligned} \quad (3)$$

which we solved numerically.

First we address the properties of the ground-state solitons with zero topological charge $m = 0$ (Fig. 1), which physically correspond to the nonlinear continuation of the lowest-order mode confined by the lattice. The power of such solitons is a monotonically decreasing function of the propagation constant [Fig. 1(b)]. The power goes to infinity at $b \to 0$ and vanishes at the upper cutoff $b_{\rm co}$ of the propagation constant. Since the lattice profile has a local minimum at $r = 0$, ground-state solitons have a small intensity dip on their top [Fig. 1(c)]. At small power levels, when $b \to b_{\rm co}$, ground-state solitons transform into linear modes guided by the first lattice ring, while at $b \to 0$, where defocusing nonlinearity dominates, the soliton di-

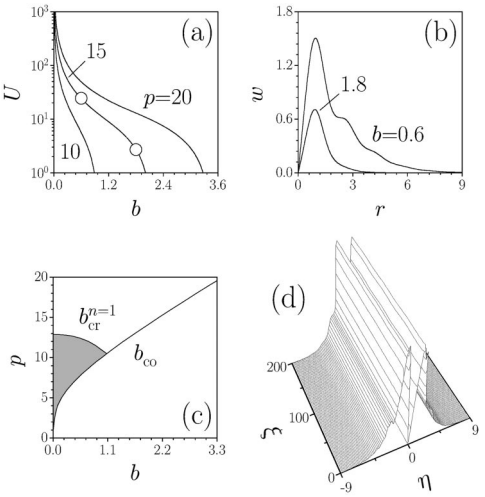

FIG. 2. (a) Power of vortex soliton with $m = 1$ versus propagation constant. (b) Amplitude profiles of solitons corresponding to points marked by circles in (a). (c) Areas of stability and instability (shaded) on the (p, b) plane for vortex solitons with $m = 1$. (d) Stable propagation of vortex with $m = 1$, $b = 0.7$ at $p = 15$ in the presence of white noise with variance $\sigma^2_{\rm noise} = 0.01$. Cut of intensity distribution at $\zeta = 0$ is shown.

ameter grows, and it covers several lattice rings [compare profiles at $b = 2.6$ and 0.5 in Fig. 1(c)]. As $b \to 0$, the soliton diameter increases dramatically while its maximal amplitude remains almost unchanged. The area of existence of ground-state solitons broadens monotonically with the growth of lattice depth [inset in Fig. 1(c)]. Linear stability analysis revealed that ground-state soliton solutions are stable in the entire domain of their existence, as expected on physical grounds. To confirm the results of the linear stability analysis we performed extensive numerical simulations using Eq. (1) with the perturbed input conditions $q|_{\xi=0} = w(r)[1 + \rho(r, \phi)]$, where $w(r)$ describes the stationary soliton, and $\rho(r, \phi)$ is the random function with Gaussian distribution and variance σ^2_{noise}. An example of stable propagation of a perturbed soliton is shown in Fig. 1(d).

We now consider VLS with topological charge $m = 1$ (Fig. 2). Note that such lattice solitons, as well as the ground-state ones, exist because defocusing nonlinearity and diffraction are balanced by the lattice that focuses radiation into the region with higher refractive index. Therefore, the Bessel lattice affords confinement of light that is impossible in a uniform defocusing medium. The power of the VLS is a monotonically decreasing function of the propagation constant [Fig. 2(a)]. There exist zero lower and positive upper cutoffs on the propagation constant. The power of the VLS diverges as $b \to 0$ and vanishes as b approaches the upper cutoff b_{co}. With an increase of the power, the VLS get wider and cover many lattice rings [Fig. 2(b)]. The existence domain of VLS with unit topological charge is displayed in Fig. 2(c). The width of the existence domain increases monotonically with growth of the lattice depth. At fixed lattice depth p, the width of the existence domain on the propagation constant reaches its maximal value for ground-state solitons and decreases with the growth of the soliton topological charge.

The central result of this Letter is that the VLS become dynamically stable in suitable domains of their existence. This is depicted in Fig. 2(c). In the plot we show the critical value of propagation constant b^n_{cr} above which no perturbations with the azimuthal index n and nonzero real part of growth rate were found. The precise structure of instability regions [shaded area in Fig. 2(c)] is complicated. There exist multiple narrow stability ''windows'' near the upper cutoff even for shallow lattices, but we do not show them here because stabilization close to the upper cutoff (where soliton transforms into the linear mode guided by the first lattice ring) is not surprising. Our simulations indicate that VLS with $m = 1$ from the shaded area in Fig. 2(c) self-destroy under the action of perturbation with the azimuthal index $n = 1$, while the corresponding instability is of oscillatory type with $\text{Re}(\delta) \ll \text{Im}(\delta)$. Decay of the unstable VLS produces either radiation or sets of ground-state solitons. When the lattice depth exceeds a critical value, of about $p_{\text{cr}} \approx 12.9$, the instability regions *cease to exist* and VLS become stable in the *entire domain* of their existence. The *stable* propagation of a vortex lattice soliton with $m = 1$ in the presence of broadband input noise is illustrated in Fig. 2(d). To illustrate that the defocusing nonlinearity is a necessary ingredient for the existence of the stable VLS, Fig. 3 shows the three-dimensional shapes of different VLS together with the linear mode supported by the lattice. Notice the differences in beam profiles introduced by the defocusing nonlinearity, in particular, the multiring structure acquired by the VLS at moderate and high powers.

Vortex lattice solitons with topological charge $m = 2$ were also studied. Their properties have much in common with properties of solitons with $m = 1$ and are summarized in Fig. 4. The instability domain is located near lower cutoff on propagation constant. It also has complex structure with separate stability windows (not shown at the plot), and its width decreases monotonically with growth of the lattice depth. Notice that vortices from the shaded area in Fig. 4(c) are affected by perturbations with azimuthal indexes $n = 1, 2$, which indicates that the spectrum of harmful perturbations enriches with the growth of the vortex topological charge. However, the important result uncovered is that for deep enough lattices a broad stability domain appears too, as shown in Fig. 4(c). An illustrative example of the propagation of a stable ring-shaped vortex soliton with $m = 2$ is presented in Fig. 4(d). We considered also vortex solitons with higher topological charges and found stability conditions. The higher the topological charge of the vortex is, the deeper the lattice required for its stabilization is. It is worth mentioning that we also found higher-order ''twisted'' vortex and ground-state modes whose field $w(r)$ alternates on successive lattice

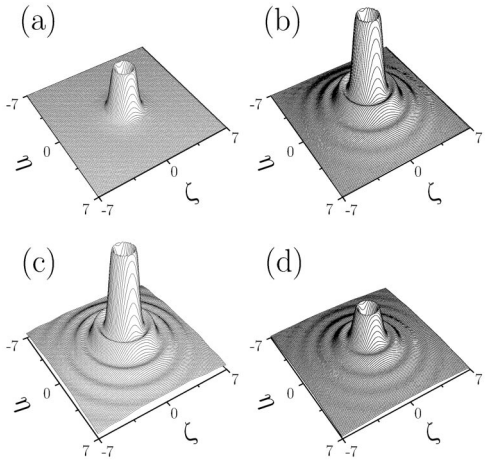

FIG. 3. Three-dimensional intensity distributions for different VLS with $m = 1$. (a) Power $U = 9$, lattice depth $p = 15$. (b) $U = 62$, $p = 15$. (c) $U = 124$, $p = 15$. (d) $U = 62$, $p = 10$. The VLS shown in (a) corresponds to the quasilinear regime. All figures are plotted with the same scale in the vertical axis.

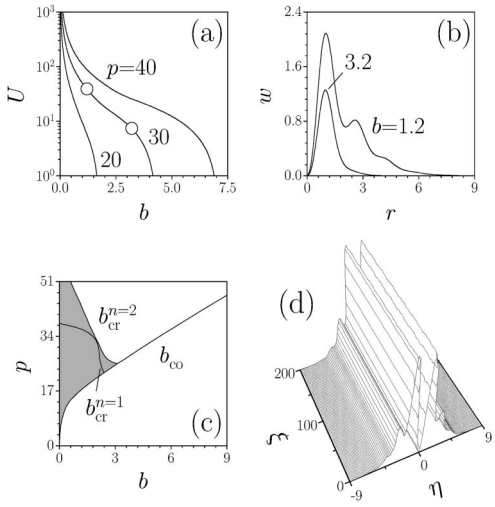

FIG. 4. (a) Power of vortex soliton with $m = 2$ versus propagation constant. (b) Amplitude profiles of solitons corresponding to points marked by circles in (a). (c) Areas of stability and instability (shaded) on the (p, b) plane for vortex solitons with $m = 2$. (d) Stable propagation of the vortex with $m = 2$, $b = 1.6$ at $p = 40$ in the presence of white noise with variance $\sigma^2 = 0.01$. Cut of intensity distribution at $\zeta = 0$ is shown.

rings, but their stability analysis is beyond the scope of this Letter. Finally, we also studied VLS in Bessel lattices imprinted in focusing nonlinear media, but we found them all to be unstable against azimuthal modulational instabilities. Such instability might be suppressed in azimuthally modulated lattices, a possibility that is open for future research.

To summarize, optical lattices induced by nondiffracting Bessel beams in media with defocusing nonlinearity have been shown to be able to support stable ring-profile vortex solitons. The existence of such bright-shaped vortex lattice solitons, which do not self-destroy by azimuthal modulational instabilities, is a rare phenomenon in physics and is an important example of the variety of phenomena afforded by Bessel optical lattices. The results reported are relevant not only for nonlinear optics but also for suitable Bose-Einstein condensates trapped in Bessel lattices with repulsive interatomic interactions. We note that the stabilization of vortex solitons by circular steplike potentials [22] and by nonlocal nonlinearities [23] has also been discovered very recently, after submission of our manuscript.

This work has been partially supported by the Government of Spain through Grant No. BFM2002-2861 and by the Ramon-y-Cajal Program.

[1] Y. S. Kivshar and G. P. Agrawal, *Optical Solitons* (Academic Press, New York, 2003); N. N. Akhmediev and A. Ankiewicz, *Solitons* (Chapman-Hall, London, 1997).

[2] V. I. Kruglov and R. A. Vlasov, Phys. Lett. **111A**, 401 (1985); L. Torner and D. V. Petrov, Electron. Lett. **33**, 608 (1997); W. J. Firth and D. V. Skryabin, Phys. Rev. Lett. **79**, 2450 (1997); J. P. Torres *et al.*, J. Opt. Soc. Am. B **15**, 625 (1998).

[3] V. Tikhonenko *et al.*, J. Opt. Soc. Am. B **12**, 2046 (1995); D. V. Petrov *et al.*, Opt. Lett. **23**, 1444 (1998); S. Minardi *et al.*, Opt. Lett. **26**, 1004 (2001); M. S. Bigelow *et al.*, Phys. Rev. Lett. **92**, 083902 (2004).

[4] G. A. Swartzlander and C. T. Law, Phys. Rev. Lett. **69**, 2503 (1992); A. W. Snyder *et al.*, Opt. Lett. **17**, 789 (1992); G. Duree *et al.*, Phys. Rev. Lett. **74**, 1978 (1995); A. V. Mamaev *et al.*, Phys. Rev. Lett. **77**, 4544 (1996); B. Luther-Davies *et al.*, J. Opt. Soc. Am. B **14**, 3045 (1997).

[5] M. Quiroga-Teixeiro and H. Michinel, J. Opt. Soc. Am. B **14**, 2004 (1997); I. Towers *et al.*, Phys. Lett. A **288**, 292 (2001); D. Mihalache *et al.*, Phys. Rev. Lett. **88**, 073902 (2002).

[6] I. Towers *et al.*, Phys. Rev. E **63**, 055601(R) (2001); D. Mihalache *et al.*, Phys. Rev. E **66**, 016613 (2002); **67**, 056608 (2003).

[7] F. Smektala *et al.*, J. Non-Cryst. Solids **274**, 232 (2000); S. Carrasco *et al.*, Opt. Lett. **27**, 2016 (2002); C. Zhan *et al.*, J. Opt. Soc. Am. B **19**, 369 (2002).

[8] S. Raghavan and G. P. Agrawal, Opt. Commun. **180**, 377 (2000).

[9] M. R. Matthews *et al.*, Phys. Rev. Lett. **83**, 2498 (1999); K. W. Madison *et al.*, Phys. Rev. Lett. **84**, 806 (2000).

[10] A. Ferrando *et al.*, Opt. Express **12**, 817 (2004).

[11] D. N. Christodoulides *et al.*, Nature (London) **424**, 817 (2003); H. S. Eisenberg *et al.*, Phys. Rev. Lett. **81**, 3383 (1998); R. Morandotti *et al.*, Phys. Rev. Lett. **83**, 2726 (1999).

[12] B. A. Malomed and P. G. Kevrekidis, Phys. Rev. E **64**, 026601 (2001).

[13] Y. V. Kartashov *et al.*, Opt. Lett. **29**, 766 (2004); **29**, 1102 (2004); Opt. Express **12**, 2831 (2004).

[14] N. K. Efremidis *et al.*, Phys. Rev. E **66**, 046602 (2002); Phys. Rev. Lett. **91**, 213906 (2003).

[15] J. W. Fleischer *et al.*, Nature (London) **422**, 147 (2003); Phys. Rev. Lett. **92**, 123904 (2004).

[16] D. Neshev *et al.*, Opt. Lett. **28**, 710 (2003); Phys. Rev. Lett. **92**, 123903 (2004).

[17] Z. Chen *et al.*, Phys. Rev. Lett. **92**, 143902 (2004).

[18] J. Yang and Z. H. Musslimani, Opt. Lett. **28**, 2094 (2003); Y. V. Kartashov *et al.*, Opt. Lett. **29**, 1918 (2004).

[19] Y. V. Kartashov *et al.*, Phys. Rev. Lett. **93**, 093904 (2004); J. Opt. B **6**, 444 (2004); Phys. Rev. E **70**, 065602(R) (2004).

[20] J. Arlt and K. Dholakia, Opt. Commun. **177**, 297 (2000); N. Chattrapiban *et al.*, Opt. Lett. **28**, 2183 (2003).

[21] A. M. Glass and J. Strait, in *Photorefractive Materials and their Applications I*, edited by P. Günter and J. P. Huignard (Springer, Berlin, 1988), pp. 237–262.

[22] S. Skupin *et al.*, Phys. Rev. E **70**, 016614 (2004).

[23] A. Yakimenko *et al.*, nlin.PS/0411024; D. Briedis *et al.*, Opt. Express **13**, 435 (2005).